

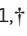



Afadin is a scaffold protein repressing insulin action via HDAC6 in adipose tissue

Morten Lundh^{1,2} , Patricia SS Petersen^{1,†} , Marie S Isidor^{1,†} , Dolly NM Kazoka-Sørensen¹, Kaja Plucińska¹, Farnaz Shamsi², Cathrine Ørskov³, Marco Tozzi¹, Erin L Brown¹, Emil Andersen¹, Tao Ma^{1,3}, Ulrich Müller⁴, Romain Barrès¹, Viggo B Kristiansen⁵, Zachary Gerhart-Hines^{1,3}, Yu-Hua Tseng² & Brice Emanuelli^{1,*} 

Abstract

Insulin orchestrates metabolic homeostasis through a complex signaling network for which the precise mechanisms controlling its fine-tuning are not completely understood. Here, we report that Afadin, a scaffold protein, is phosphorylated on S1795 (S1718 in humans) in response to insulin in adipocytes, and this phosphorylation is impaired with obesity and insulin resistance. In turn, loss of Afadin enhances the response to insulin in adipose tissues via upregulation of the insulin receptor protein levels. This happens in a cell-autonomous and phosphorylation-dependent manner. Insulin-stimulated Afadin-S1795 phosphorylation modulates Afadin binding with interaction partners in adipocytes, among which HDAC6 preferentially interacts with phosphorylated Afadin and acts as a key intermediate to suppress insulin receptor protein levels. Adipose tissue-specific Afadin depletion protects against insulin resistance and improves glucose homeostasis in diet-induced obese mice, independently of adiposity. Altogether, we uncover a novel insulin-induced cellular feedback mechanism governed by the interaction of Afadin with HDAC6 to negatively control insulin action in adipocytes, which may offer new strategies to alleviate insulin resistance.

Keywords adipocyte; adipose tissue; Afadin; HDAC6; insulin

Subject Categories Metabolism; Post-translational Modifications, Proteolysis & Proteomics

DOI 10.15252/embr.201948216 | Received 2 April 2019 | Revised 21 May 2019 | Accepted 31 May 2019 | Published online 2 July 2019

EMBO Reports (2019) 20: e48216

Introduction

Adipose tissue dysfunction in obesity is being increasingly recognized as one of the main culprits of insulin resistance [1], which,

together with an inability to compensate by increased insulin secretion, constitutes the pathogenic hallmarks underlying type 2 diabetes mellitus (T2DM). In agreement with this notion, reduction of white adipose tissue (WAT) mass (especially visceral) improves insulin sensitivity and metabolic homeostasis [1,2]. Alternatively, ectopic or genetic manipulation of adipose tissue function also leads to metabolic improvements [3–5]. Hypertrophic adipose tissue undergoes a chronic inflammatory state associated with increased fibrosis, impaired adipokine secretion [6], and secretion of pro-inflammatory cytokines such as TNF- α [7], which induces insulin resistance in adipose tissue, muscle, and liver [8,9]. Intracellularly, impaired adipocyte insulin signaling results in reduced uptake of free fatty acids and glucose and increased lipolysis, leading to an overall raise in circulating fatty acids [10], which further blunts insulin action in other organs [11]. Thus, strategies to improve adipose tissue function and insulin action in adipocytes may lead to new therapeutic approaches to alleviate insulin resistance and T2DM.

In cells, insulin action is mediated by a complex network of signaling events regulating key processes such as substrate uptake and utilization, protein synthesis, cell growth, and differentiation [12]. Not surprisingly, insulin signaling is tightly regulated by several different inhibitory steps such as receptor internalization, inhibitory phosphorylation events, phosphatase activities, and pseudosubstrate docking, allowing precise control and fine-tuning of the signaling cascades; notably several of these inhibitory steps are dysregulated in states of insulin resistance [13]. Aiming at further deciphering the molecular mechanisms mediating insulin/IGF-1 signal transduction, we identified Afadin as a novel intermediate in this pathway [14]. Afadin is an intracellular adaptor protein localized near the plasma membrane at adherens junctions, which is encoded by the *Mllt4* gene with two main isoforms in the mouse: I-Afadin (~ 205 kDa) and S-Afadin (~ 190 kDa) [15]. Afadin contains nine domains including two Ras-associated domains, a PDZ domain, and an F-actin-binding domain, presumably important for the many

1 Faculty of Health and Medical Sciences, Novo Nordisk Foundation Center for Basic Metabolic Research, University of Copenhagen, Copenhagen, Denmark

2 Joslin Diabetes Center, Harvard Medical School, Boston, MA, USA

3 Department of Biomedical Sciences, Faculty of Health and Medical Sciences, University of Copenhagen, Copenhagen, Denmark

4 Department of Molecular and Cellular Neuroscience, Dorris Neuroscience Center, The Scripps Research Institute, La Jolla, CA, USA

5 Department of Surgical Gastroenterology, Hvidovre Hospital, Hvidovre, Denmark

*Corresponding author. Tel: +45 2381 4735; E-mail: emanuelli@sund.ku.dk

†These authors contributed equally to this work

functions of Afadin. In addition to its involvement in cell–cell adhesion, Afadin regulates cell migration, survival, proliferation, and differentiation of fibroblasts, and epithelial and endothelial cells, and more than 20 interaction partners have been described [15,16]. Interestingly, recent work has also demonstrated a role for Afadin in regulating transcription by sequestering the FOXE1 transcription factor [17], underlying that Afadin is a multifunctional protein. Notably, insulin-growth factor (IGF)-1-induced phosphorylation of Afadin (S1718) was shown to promote breast cancer cell migration *in vitro* [18]. However, the role of Afadin in modulating insulin action and metabolic homeostasis is not known.

Here, we identify I-Afadin as a *bona fide* target of the insulin signaling pathway in adipose tissues and in preadipocytes and mature adipocytes from mouse and human. We show that Afadin is a negative regulator of insulin action *in vitro* and *in vivo*, and through the identification of Afadin's protein interactome, we uncover histone deacetylase 6 (HDAC6) as a molecular link between Afadin and insulin signaling, controlling glucose homeostasis in obese mice. These data reveal a novel cellular feedback mechanism to control insulin action, which may provide new therapeutic opportunities for insulin resistance-related disorders.

Results

Insulin promotes the phosphorylation of Afadin on S1795 (human S1718)

Using a quantitative phosphoproteomic analysis to identify novel mediators of insulin/IGF-1 signaling, we found that the phosphorylation of Afadin at the serine residue S1795 was one of the most pronounced events following IGF-1 stimulation [14]. Notably, S1795 was the only Afadin residue with substantial increased phosphorylation in response to IGF-1 (Fig 1A). Since our initial study was performed in preadipocytes using IGF-1 stimulation, we first demonstrated that Afadin was phosphorylated at S1795 by insulin in brown preadipocytes (Fig 1B) and mature (Fig 1C) adipocytes. Insulin-stimulated Afadin phosphorylation occurred in a dose- and time-dependent manner (Figs 1B and EV1A). Insulin was also capable of inducing Afadin S1718 phosphorylation (corresponding to mouse

S1795) in immortalized human white and brown adipocytes [19] (Fig 1D) and in isolated primary human adipocytes (Fig 1E). In accordance with the regulation of Afadin S1795 phosphorylation in breast cancer cells by IGF-1 [18], we showed that insulin-stimulated phosphorylation of Afadin in adipocytes was primarily mediated downstream of Akt activation (Fig EV1B). Whether Akt directly phosphorylates Afadin remains to be determined. *In vivo*, we observed a 4-fold induction of Afadin S1795 phosphorylation in mouse brown adipose tissue (BAT) following insulin stimulation (Fig 1F). Importantly, we also detected an increase in phosphorylation of Afadin S1795 in BAT and subcutaneous white fat (sWAT), following re-feeding in mice (Figs 1G and EV1C), indicating the physiological relevance of this event. Since Afadin S1795 phosphorylation has been reported in the liver following insulin stimulation by quantitative mass spectrometry [20], we compared the ratios of phosphorylated to total Afadin levels in BAT, sWAT, and liver from mice injected with insulin and found this ratio to be higher in fat depots as compared to the liver (Fig EV1D), suggesting a predominant role for Afadin phosphorylation in adipose tissues compared to liver. Lastly, to address the potential involvement of this phosphorylation event in pathophysiological situations, we investigated how Afadin phosphorylation is affected by insulin resistance and obesity. We observed that insulin-stimulated phosphorylation of Afadin S1795 was completely abolished in BAT from diet-induced obese mice, despite residual pAkt levels (Figs 1H and EV1E). Interestingly, Afadin protein abundance was also reduced in BAT from mice on HFD compared to chow (Figs 1H and EV1E), indicating that both Afadin phosphorylation and protein levels are regulated by diet. We then explored Afadin phosphorylation in cultured stromal vascular fraction (SVF) from either lean, obese, or T2DM human subjects [21], following insulin stimulation. While insulin was able to induce the S1718 phosphorylation of Afadin in SVF from lean subjects, this induction was weakened in the SVF from both obese and T2DM subjects despite intact Akt phosphorylation [21]; (Fig 1I).

Collectively, these data show that Afadin is a *bona fide* substrate of the insulin signaling pathway in preadipocytes and mature adipocytes and adipose tissues, and the ability of insulin to induce the phosphorylation of Afadin at S1795/S1718 is reduced in both animals and human cells under conditions of obesity and insulin resistance.

Figure 1. Afadin is phosphorylated at serine 1795/1718.

- A Phosphorylation of Afadin at serine 1795 (marked with asterisk) revealed by quantitative phosphoproteomic analysis in brown preadipocytes stimulated with IGF-1 for 5 min. Table shows eight identified phosphopeptides belonging to Afadin, where the phosphorylated residue is underlined and highlighted in bold.
- B Immunoblotting and quantification of brown preadipocytes (WT-1) stimulated with insulin at different doses for 5 min ($n = 3$). The molecular weight corresponded to the I-Afadin isoform.
- C Immunoblotting and quantification of mature brown adipocytes (WT-1) stimulated with insulin (100 nM) for 5 min ($n = 4$).
- D Immunoblotting of immortalized human mature white and brown adipocytes stimulated with insulin for 5 min ($n = 3$).
- E Immunoblotting and quantification of primary human mature white adipocytes stimulated with insulin for 5 min ($n = 3$).
- F Immunoblotting and quantification of isolated brown adipose tissue (BAT) from male C57BL/6J mice injected with 5 U insulin for 5 min ($n = 4-6$).
- G Quantification of immunoblotting of isolated BAT, subcutaneous white adipose tissue (sWAT), and visceral white adipose tissue (vWAT) from male C57BL/6J mice after fasting or re-feeding for 2/6 h ($n = 6$).
- H Immunoblotting and quantification of total and Afadin S1795 phosphorylation in adipose tissue depots from 12-week-old C57BL/6 male mice fed with either chow (CD) or high-fat diet (HFD) for 6 weeks injected with vehicle or insulin ($n = 6$).
- I Immunoblotting and quantification of Afadin S1718 phosphorylation in human stromal vascular fractions (SVF) from lean, obese, or type 2 diabetic (T2DM) subjects stimulated or not with insulin ($n = 6$).

Data information: Representative Western blots are shown. Data are presented as means + SEM; Student's unpaired t-test and ANOVA with Tukey or Dunnett's *post hoc* test: * $P < 0.05$, ** $P < 0.01$, *** $P < 0.001$, NS = no significance.

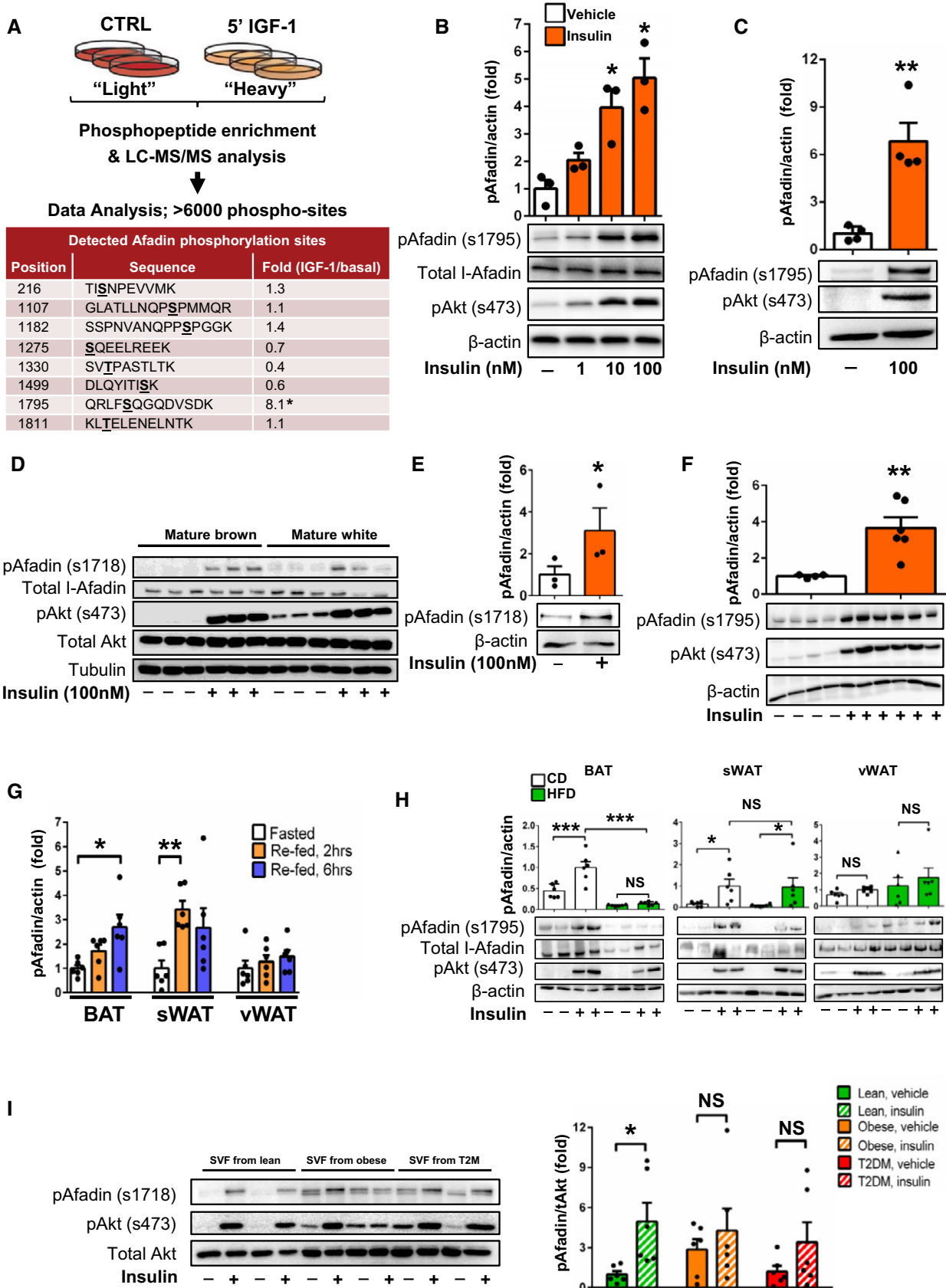


Figure 1.

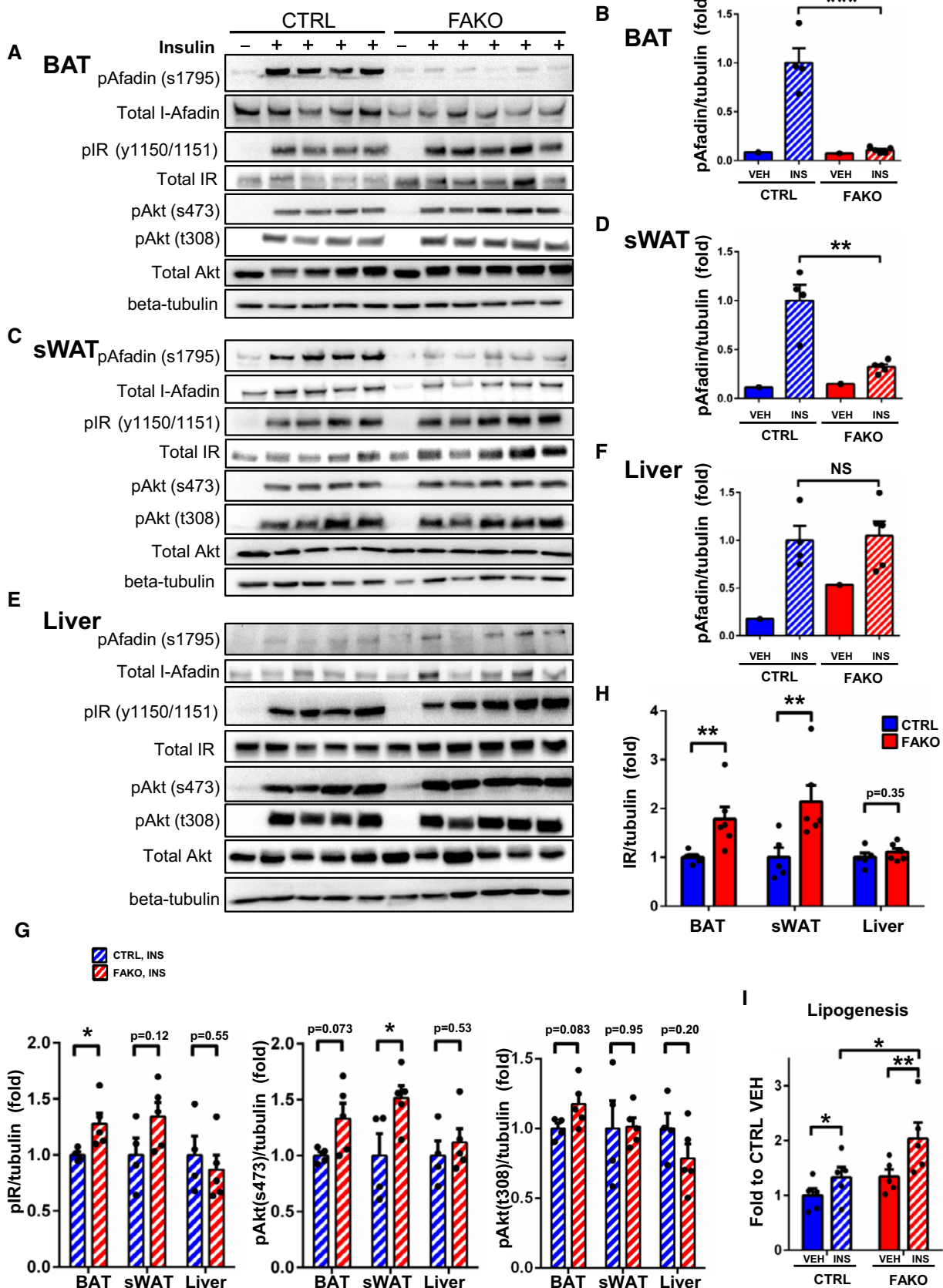


Figure 2.

Figure 2. Insulin action is improved in adipose tissue of mice with adipose tissue-specific ablation of Afadin.

Protein lysates from 10- to 13-week-old CTRL and FAKO (*Mllt4*^{-/-}) mice following retro-orbital injection of insulin (1 U) were immunoblotted and quantified.

- A, B BAT; Immunoblotting and quantification of Afadin S1795 phosphorylation (*n* = 4–5).
 C, D sWAT; Immunoblotting and quantification of Afadin S1795 phosphorylation (*n* = 4–5).
 E, F Liver; Immunoblotting and quantification of Afadin S1795 phosphorylation (*n* = 4–5).
 G Quantifications of phosphorylated insulin receptor β and phosphorylated Akt across the three tissues (*n* = 4–5).
 H Quantifications of total IR β /tubulin in BAT, sWAT, and liver (*n* = 5–6).
 I Insulin-induced lipogenesis in isolated mature adipocytes from CTRL and FAKO (*Mllt4*^{-/-}) mice (*n* = 5).

Data information: Data are presented as means + SEM; ANOVA with Tukey or Dunnett's *post hoc* test: **P* < 0.05, ***P* < 0.01, ****P* < 0.001, NS = no significance.

Afadin is a negative regulator of intracellular insulin signaling and insulin action *in vivo*

To assess the function of Afadin in adipose tissue, we generated a Fat-Afadin-Knock-Out (FAKO) mouse model using the adiponectin-driven Cre recombinase to specifically ablate *Mllt4* (encoding Afadin) in adipose tissues (Fig EV2A), which was confirmed on mRNA (Fig EV2B and C) and protein (Figs 2A and EV2D) levels. We did not observe any change in adipose tissue weights (Fig EV2E), adipose tissue triglyceride content (Fig EV2F), food intake (Fig EV2G), nor in the expression of key adipocyte genes—including *IR* mRNA—(Fig EV2H) between FAKO and control littermates. However, we found that deletion of Afadin directly influences insulin signaling. Insulin injection in control mice led to a robust induction of Afadin S1795 phosphorylation in BAT and sWAT, and this was completely abolished in BAT of FAKO mice (Fig 2A and B) and reduced by 75% in sWAT of FAKO animals (Fig 2C and D), whereas insulin-induced phosphorylation of Afadin in the liver was similar in control littermates and FAKO animals (Fig 2E and F). Interestingly, a twofold increase in IR levels was observed in both BAT and sWAT from FAKO mice compared to control littermates (Fig 2A, C, E and H). The regulation of IR protein abundance is likely posttranscriptional, given unchanged *IR* mRNA levels (Fig EV2H) in adipose tissues from FAKO and control animals. This was accompanied by a 27% increased phosphorylation, and thus activation, of the IR in BAT of FAKO mice compared to control littermates, and a trend toward increased Akt phosphorylation in BAT, and a significant increase (51%) in phosphorylated Akt S473 in sWAT, of FAKO mice compared to control animals, respectively (Fig 2G). No difference in the levels of phosphorylation of IR or Akt was observed in the liver in these conditions (Fig 2G). Performing an ambulant time-response insulin stimulation experiment using a lower dose of insulin, we confirmed that the action of insulin was enhanced selectively in BAT and sWAT of FAKO mice after 15 min of insulin stimulation, and no difference was observed after 1 or 2 h of stimulation (Fig EV2I). The enhanced insulin

signaling observed in Afadin-deficient adipose tissue was associated with a 53% increase in insulin-stimulated lipogenesis in primary adipocytes isolated from FAKO mice compared to control littermates (Fig 2I). Collectively, our *in vivo* data suggest that Afadin is a negative regulator of insulin action in adipose tissue, likely by controlling IR protein availability and thereby its downstream intracellular signaling.

Afadin-mediated weakening of insulin action is cell-autonomous and occurs in a phosphorylation-dependent manner

To further investigate the mechanisms by which Afadin regulates insulin signaling, we used CRISPR/nCas9 technology [22] to generate two different models of loss of Afadin: an isolated Afadin-Knock-Out (KO) clone (*Afdn*-KO), and a bulk cell population composed of both wild-type (WT) and Afadin KO cells (Figs 3A and EV3A). Examination of these two models showed that loss of Afadin did not affect cell differentiation in a negative manner, as exemplified by similar triglyceride accumulation, and comparable expression levels of mature adipocyte marker genes, with the exception of a modest potentiation of the early differentiation regulators *C/ebp- α* and *C/ebp- β* expression (Figs 3B and EV3B). Despite equivalent differentiation, we found that loss of Afadin resulted in enhanced response to insulin in mature adipocytes, recapitulating our *in vivo* observations at the cellular level. Indeed, a 90% increase in phosphorylation of Akt was observed in response to insulin in differentiated Afadin KO adipocytes compared to wild-type control cells (Fig 3C and D). Importantly, re-expression of a FLAG-tagged version of wild-type Afadin (Fig EV3C) restored insulin-stimulated phosphorylation of Akt to the level of WT cells (Fig 3C and D), demonstrating that Afadin is a negative regulator of insulin action in adipocytes. By contrast, enhanced insulin-stimulated phosphorylation of Akt was preserved in cells complemented with a non-phosphorylatable S1795A Afadin mutant form (Fig 3C and D), demonstrating that phosphorylation of Afadin at this residue is necessary to negatively impact insulin action. Concomitantly with the enhanced insulin-

Figure 3. Cell-intrinsic modulation of insulin action by Afadin depends on S1795 phosphorylation.

- A CRISPR/nCas9-mediated ablation of Afadin protein levels in a clonal cell population termed *Afdn*-KO.
 B Oil red O staining and gene expression of selected adipogenic genes in WT-1 and *Afdn*-KO differentiated adipocytes (*n* = 3).
 C Wild-type, *Afdn*-KO, and *Afdn*-KO with re-expression FLAG-tagged WT I-Afadin or a non-phosphorylatable form (S1795A) stimulated with vehicle or insulin (*n* = 4) for Immunoblotting.
 D Quantification of insulin-induced Akt phosphorylation from immunoblots.
 E, F Real-time measurement (E) and quantification (F) of insulin-induced fatty acid uptake (*n* = 4).

Data information: Representative Western blots are shown. Data are presented as means + SEM; Student's unpaired *t*-test and ANOVA with Tukey or Dunnett's *post hoc* test: **P* < 0.05, ***P* < 0.01, ****P* < 0.001, NS = no significance.

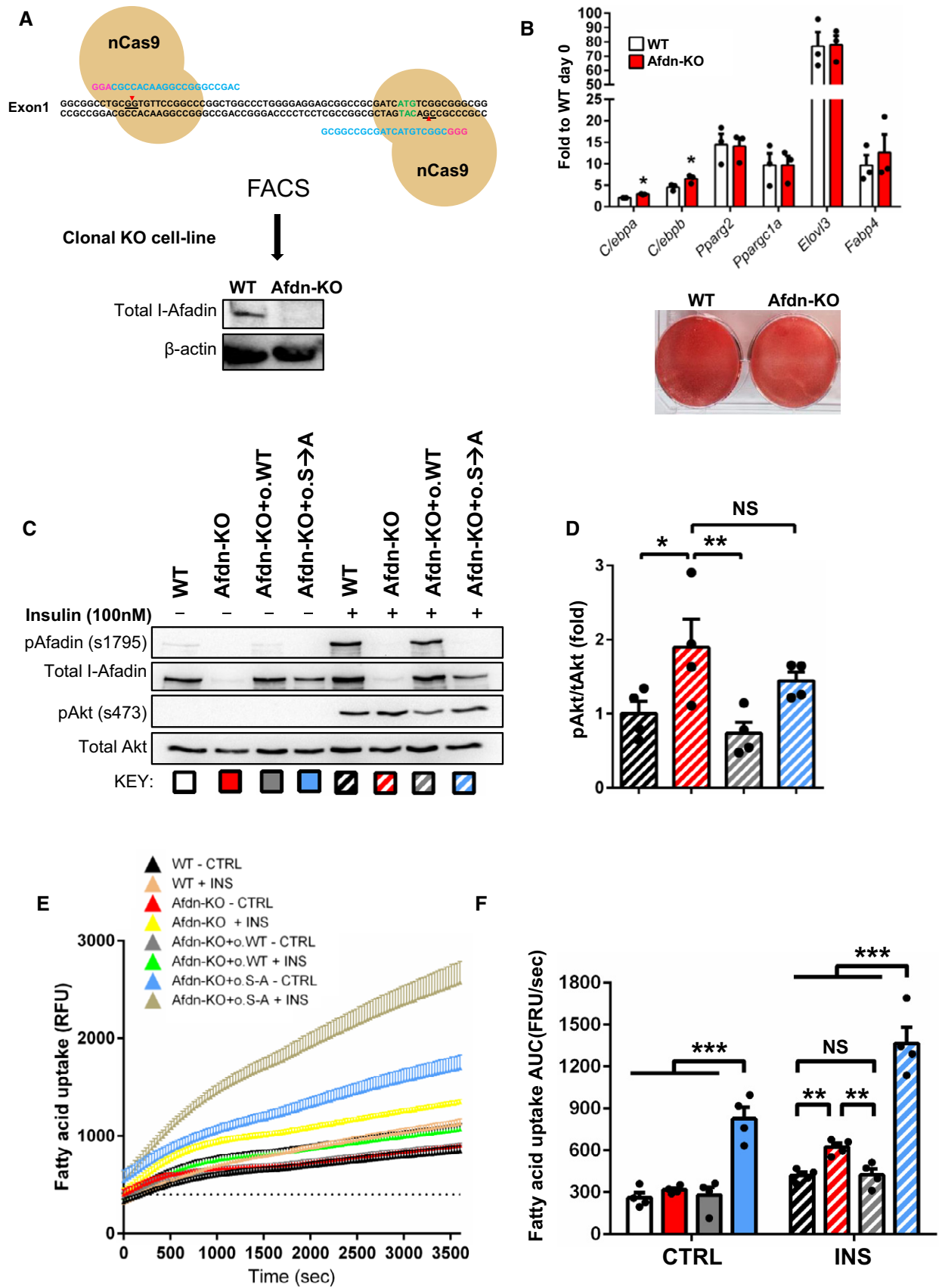


Figure 3.

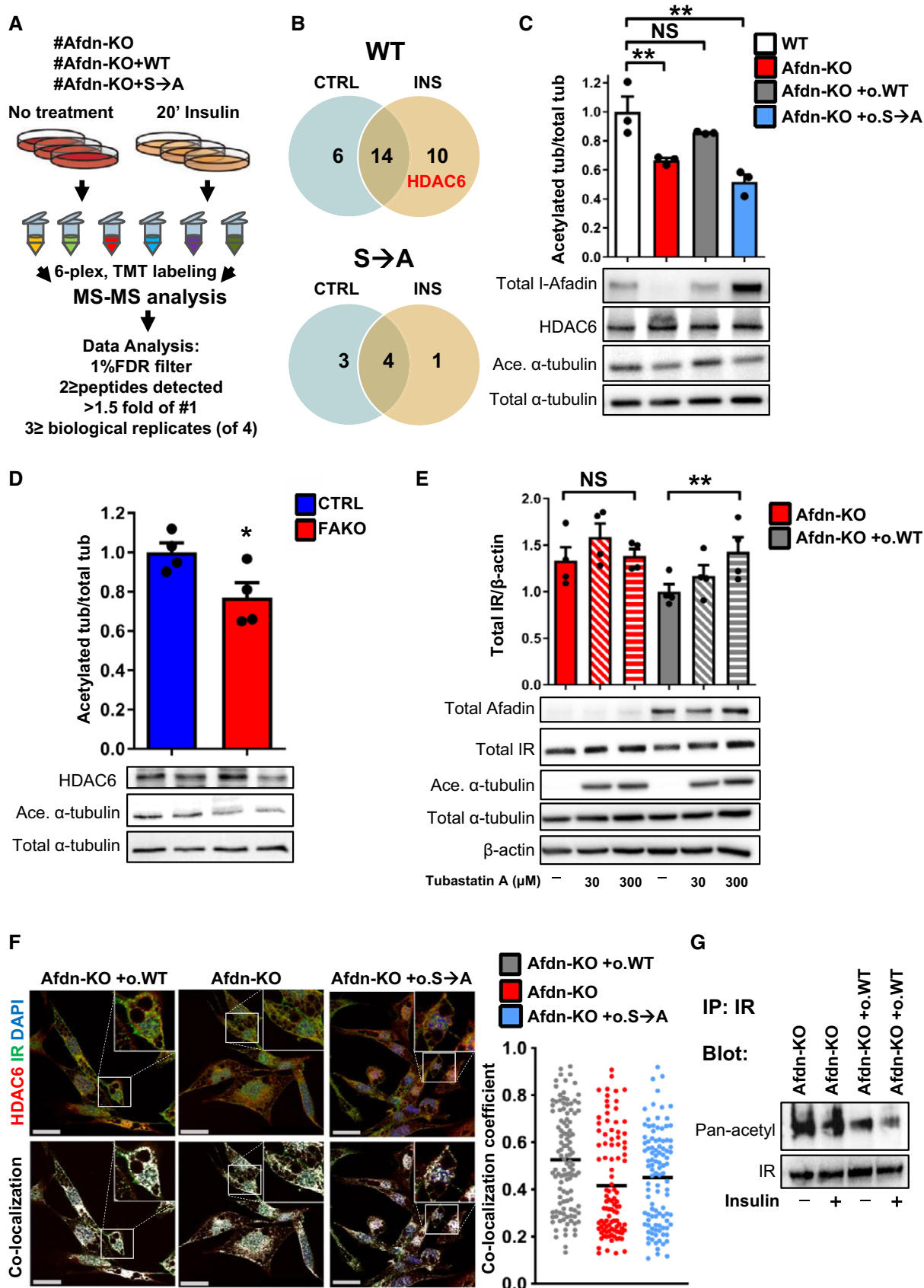


Figure 4.

Figure 4. Afadin interacts with HDAC6 and modulates its activity to regulate IR levels.

- A Experimental strategy for the identification of insulin- and S1795-dependent Afadin binding partners.
 B Venn diagrams illustrating the number of proteins interacting with WT Afadin or S1705A Afadin upon insulin stimulation for 20 min ($n = 4$).
 C Acetylated α -tubulin levels in cell lines ($n = 3$).
 D Acetylated α -tubulin levels in isolated mature adipocytes from CTRL and FAKO ($Mlt4^{-/-}$) mice ($n = 4$).
 E IR abundance measured by immunoblotting following 4 h preincubation with the HDAC6 inhibitor (Tubastatin A) in differentiated adipocytes exposed to insulin (100 nM) stimulation for 15 min ($n = 4$).
 F Immunolocalization of IR (green) and HDAC6 (red) in Afdn-KO and Afdn-KO with re-expression FLAG-tagged WT Afadin or S1795A Afadin in mature adipocytes stimulated with insulin. Nuclei were stained with DAPI (blue). Co-localization was detected by the appearance of white pixels where the red and green overlap. Scale bars: 25 μ m. Representative images are shown. The ratio of IR co-localized with HDAC6 (Mandler's co-localization coefficient) was quantified (98–112 individual cells from two independent experiments).
 G Immunoprecipitation of IR followed by immunoblotting using an anti-acetyl-Lys antibody in adipocytes lacking Afadin or re-expressing Afadin, with or without insulin stimulation ($n = 1$).

Data information: Representative Western blots are shown. Data are presented as means + SEM; Student's unpaired t-test and ANOVA with Tukey or Dunnett's *post hoc* test: * $P < 0.05$, ** $P < 0.01$, NS = no significance.

induced Akt phosphorylation in cells lacking Afadin, insulin led to increased fatty acid uptake in Afdn-KO cells compared to controls. This effect was restored by the re-expression a WT Afadin (Fig 3E and F). Surprisingly, we observed a pronounced fatty acid uptake in adipocytes expressing the S1795A mutant; both under basal and insulin-stimulated states, indicating a gain-of-function (Fig 3E and F).

Thus, we show that Afadin provides a cell-autonomous negative regulation on insulin action in adipocytes *via* a single S1795 phosphorylation site, without affecting adipogenesis.

Afadin modulates insulin receptor levels through its interaction with HDAC6

To pinpoint the molecular intermediates of Afadin's regulation of insulin action, we aimed at determining the Afadin protein interactome in adipocytes. We performed Afadin co-immunoprecipitation (co-IP) followed by quantitative mass spectrometry using differentiated cells lacking Afadin (Afdn-KO), and in cells re-expressing WT Afadin or S1795A Afadin, upon stimulation or not with insulin (Fig 4A). A total of 30 interacting partners were identified; six were bound to Afadin only at basal state, 14 bound irrespective of insulin stimulation, and 10 were found to bind to Afadin upon insulin stimulation (Figs 4B and EV4A). Among the identified proteins were actin and Sorbs1 (Fig EV4A), which have previously been described as Afadin binding partners in other cell types [23,24]. Eight proteins were able to bind to the non-phosphorylatable form of Afadin, of which only one was detected in conditions of insulin stimulation (Figs 4B and EV4A). Thus, the loss of this specific phosphorylation site has dramatic effects on the binding of interacting proteins with Afadin.

Among the 10 proteins bound to Afadin preferentially in insulin-stimulated conditions, we identified HDAC6, which was recently shown to modulate adiposity and insulin sensitivity as adipose tissue-specific loss of HDAC6 promoted obesity and insulin resistance in mice [25]. The interaction between HDAC6 and Afadin was confirmed by immunoprecipitation followed by Western blotting (Fig EV4B). HDAC6 belongs to the family of classical HDACs, but is rather atypical due to its cytosolic residency [26]. It has both enzymatic- and non-enzymatic-dependent functions and has been implicated in cell-cell interactions and in the regulation of the cytoskeleton by deacetylation of α -tubulin [26]. As HDAC6 is the predominant enzyme responsible for

deacetylating α -tubulin [27], we examined whether Afadin interaction with HDAC6 would modulate HDAC6 activity by assessing acetylated α -tubulin levels. Interestingly, the ratio of acetylated α -tubulin/total α -tubulin was decreased in Afdn-KO cells compared to WT cells, and this ratio was restored to the level of WT cells by re-expression of the WT form of Afadin, but not of the S1795A mutant in Afdn-KO cells (Fig 4C). We observed a similar reduction in α -tubulin acetylation in primary adipocytes from FAKO mice compared to CTRL (Fig 4D). Total levels of HDAC6 protein were unaffected by Afadin ablation (Fig 4C and D). These data suggest that Afadin regulates the acetylation levels of α -tubulin, likely by modulating HDAC6 activity and/or intracellular localization, and that this regulation is dependent on insulin stimulation of Afadin S1795 phosphorylation.

Our data suggest that the enhanced insulin action resulting from Afadin depletion is due to increased IR availability. Thus, to test whether the modulation of HDAC6 activity may be involved in the upregulation of IR caused by Afadin ablation, we assessed IR protein levels in Afdn-KO cells upon ablation of HDAC6 protein or activity. We found that siRNA-mediated reduction in HDAC6 protein led to a moderate upregulation of total insulin receptor (IR) protein levels in WT, but not in Afadin-ablated adipocytes (Fig EV4C). Moreover, to investigate the role of HDAC6 activity in this process, we used the HDAC6-selective inhibitor Tubastatin A [28]. HDAC6 inhibition, monitored by the increase in acetylated- α -tubulin (Fig 4E), significantly increased total IR levels in Afadin KO cells re-expressing wild-type Afadin to the levels observed in Afadin KO cells, where Tubastatin A did not induce any further increase (Fig 4E). To test the potential role of Afadin in regulating the cellular localization of HDAC6, we performed immunocytochemistry in mature adipocytes to investigate any potential spatial overlap of the IR and HDAC6. As shown in Fig 4F, the co-localization of IR with HDAC6 was greater in insulin-stimulated mature adipocytes expressing WT Afadin compared to either adipocytes lacking Afadin or expressing the non-phosphorylatable form (Fig 4F), suggesting that insulin-mediated phosphorylation of Afadin facilitates IR and HDAC6 co-localization. Furthermore, immunoprecipitation of the IR followed by pan-acetylation immunoblotting revealed increased acetylation levels in adipocytes lacking Afadin, as compared to adipocytes re-expressing Afadin (Fig 4G).

Collectively, our findings indicate that the HDAC6-mediated regulation of IR abundance in adipocytes depends on the presence

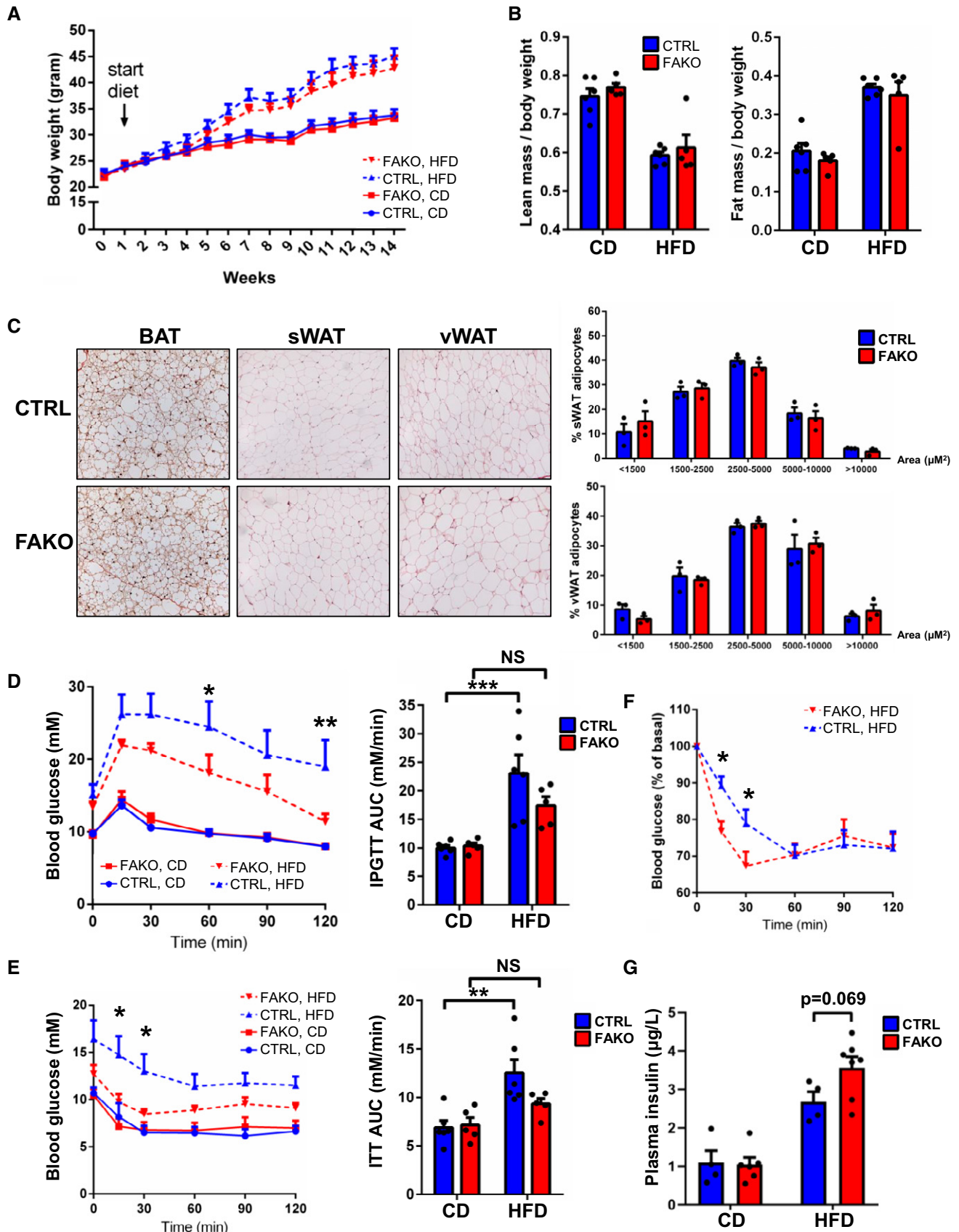


Figure 5.

Figure 5. Ablation of Afadin in adipose tissue improves diet-induced insulin resistance despite no changes in body weight or fat mass.

Seven-week-old CTRL and FAKO (*Mllt4^{-/-}*) mice were given control diet (CD) or high-fat diet (HFD) for 16 weeks ($n = 5-6$).

- A Body weight.
- B Body composition.
- C Sirius Red staining of representative embedded BAT, sWAT, and vWAT from mice on HFD and quantification of adipocyte areas ($\sim 1,000$ adipocytes/genotype).
- D IPGTT after 12 weeks of diet and AUC.
- E, F ITT after 13 weeks of diet and AUC (E) and normalized to basal insulin (F).
- G Plasma insulin levels 5 min after an IPGTT performed after 18 weeks of diet.

Data information: Data are presented as means + SEM; ANOVA with Tukey or Dunnett's *post hoc* test: * $P < 0.05$, ** $P < 0.01$, *** $P < 0.001$, NS = no significance.

of Afadin, and suggest that the upregulation of IR levels in Afadin depleted adipocytes and adipose tissue results from changes in Afadin-dependent HDAC6 activity and localization affecting the acetylation status of the IR.

Adipose tissue-specific depletion of Afadin improves metabolic homeostasis in obese mice

Since deletion of Afadin increases insulin action via, at least in part, upregulation of IR protein levels, we investigated whether Afadin deletion in adipose tissue would be protective in the context of diet-induced insulin resistance. FAKO mice and control littermates were challenged with HFD or maintained on a control diet (CD). Weight gain (Fig 5A), body composition (Figs 5B and EV5A), and food intake (Fig EV5B) were comparable between FAKO mice and their control littermates, independently of diet. Despite the known role of Afadin in cell–cell contacts, no obvious differences in adipose tissue morphology or adipocyte size were observed in BAT, sWAT, and vWAT histology (Fig 5C). However, fasted and random-fed blood glucose levels were significantly increased in control littermates on HFD compared to CD, but not in FAKO mice (Fig EV5C). In addition, glucose clearance (Fig 5D) and insulin responsiveness (Figs 5E and F, and EV5D) were improved in FAKO mice compared to control littermates, when mice were placed on HFD. Plasma insulin levels trended to be increased in FAKO mice on HFD compared to control littermates 5 min after glucose administration, although it did not reach statistical significance ($P = 0.069$, Fig 5G). Calculation of the slopes from time 0 to 30 min from the ITT curves followed by hierarchical modeling revealed a higher glucose disposal rate in FAKO mice compared to control littermates ($P = 0.0447$). Qualitative assessment of crown-like structures as an indicator of inflammation in the adipose tissues did not reveal any overt differences (Fig EV5E), suggesting that the improved metabolic homeostasis appeared without changes in adipose tissue inflammation. This happened without major apparent changes in the expression of key genes involved in mitochondrial oxidation, fatty acid utilization, lipid droplets, and lipid synthesis (Fig EV6).

Thus, our data indicate that adipose tissue-specific ablation of Afadin protects against obesity-induced metabolic imbalance, despite similar weight gain and adiposity.

Discussion

In the present study, we describe the scaffold protein Afadin as a novel element of the insulin signaling transduction pathway in adipocytes and uncover a novel mechanism by which insulin action

is negatively controlled at the level of its receptor by Afadin, via its interaction with HDAC6.

The role of Afadin was originally described as an actin-binding protein localized to cadherin-based adherens junctions [23], and several studies have demonstrated Afadin's function as a mediator of tight adherens junctions crucial for cell–cell adhesion, cell migration, and cell polarization [16]. Our results do not indicate that Afadin controls cell–cell contacts and tissue integrity in adipose tissue. Indeed, we did not observe any changes in adipocyte size or adipose tissue morphology in FAKO mice, indicating normal adipose tissue composition. Consistent with this observation, evidence of the presence of adherens junctions in adipocytes and adipose tissue is lacking [29–31]. Thus, the major function of Afadin in adipose tissue is likely not related to cell–cell contact. Instead, our data indicate that ablation of Afadin in adipocytes increases IR protein and enhances insulin signaling and insulin action, suggesting that Afadin acts as a negative regulator of the insulin signal transduction pathway. Our results also indicate that phosphorylation of Afadin at S1795 plays an important role in regulating its function. Indeed, we found that Afadin is phosphorylated at S1795 (human S1718) by insulin in both preadipocytes and mature adipocytes from mouse and human and in adipose tissues. We further demonstrate that the ability of Afadin to negatively control intracellular insulin signaling depends on its phosphorylation on S1795.

Interestingly, our data describing the Afadin's interactome in adipocytes under basal and insulin-stimulated conditions reveal that insulin modulates the interaction of Afadin with several binding partners. Indeed, insulin reduced the interaction of Afadin with six proteins whereas it enhances the binding of 10 others, including actin and HDAC6. Thus, in the adipocyte, Afadin is likely to function as a scaffold protein mediating insulin-induced localization of several proteins resulting in the regulation of insulin action according to the following working model: Insulin stimulates the phosphorylation of the IR–Akt axis leading to Akt-mediated phosphorylation of Afadin at S1795. This phosphorylation recruits HDAC6 through its binding to Afadin, which reduces insulin signaling by decreasing the availability of total IR in a deacetylase-dependent manner, thus providing a negative feedback mechanism (Fig 6A). However, in cells deprived of Afadin or with reduced Afadin phosphorylation levels (e.g., models of mild insulin resistance), HDAC6 is not recruited to Afadin and binds preferentially to other targets such as α -tubulin instead (reflected by the decreased acetylated α -tubulin levels in Afadin depleted adipocytes). Consequently, HDAC6 is not closely associated to the IR–Akt axis and the negative feedback is compromised, resulting in an increase in the amount of IR causing enhanced activation of the IR–Akt pathway and increased insulin action (Fig 6B). Interestingly,

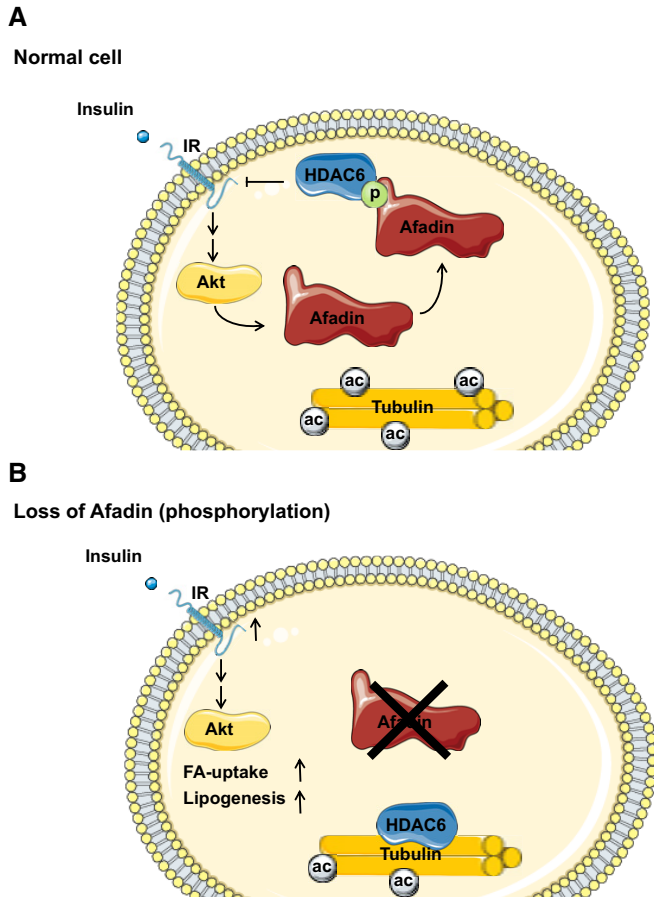


Figure 6. Proposed model of the regulation of insulin action by Afadin.

- A** Insulin stimulates the IR-Akt pathway activating Akt which phosphorylates Afadin at S1795. This allows the docking of HDAC6, which subsequently inhibits IR-Akt signaling through regulation of total IR protein in a deacetylase-dependent manner.
- B** Adipocytes lacking Afadin have increased IR availability due to the loss of HDAC6-mediated inhibition, consequently enhancing insulin signaling and action.

Sorbs1, which has previously been shown to interact with the IR in a human hepatoma cell-line [32], was identified as an Afadin interactant in our Afadin co-IP experiment, indicating a potential spatial localization overlap between Afadin, HDAC6, and IR. Our data further suggest that the IR is prone to (de)acetylation, and that acetylation of the IR depends on the presence of Afadin. Notably, even though no acetylation site has yet been mapped on the IR, the IGF-1R is acetylated on lysine 1088 [33], which is a highly conserved residue between the IGF-1R and the IR (lysine 1112) [34]. Although we cannot exclude that IGF-1R acetylation is also detected in this IP (as part of a hybrid complex with IR), and/or that other acetylation events participate in this regulation, our data raise the interesting possibility that IR levels are regulated via acetylation at this specific residue. Further experiments are needed to dissect the mechanisms by which Afadin-HDAC6 regulates acetylation and downregulation of the insulin receptor and the functional relevance of the Afadin/HDAC6/IR axis remains to be demonstrated. HDAC6 has recently been shown to regulate lipid

droplet formation and thereby lipid storage in adipocytes affecting whole-body metabolism [25], substantiating the importance of HDAC6 in adipose tissue biology.

In agreement with an involvement of Afadin in a regulatory feedback loop impeding insulin action in adipocytes, adipose tissue-specific loss of Afadin improves glucose and insulin tolerance in obese mice, without any changes in adiposity. Overexpression of the insulin receptor *in vitro* potentiates insulin signaling [35], and analogous to our findings, ablation of the E3 ubiquitin ligase March1 was shown to increase insulin action by increasing IR protein availability [36], demonstrating that an increase in insulin receptor levels is sufficient to enhance its signaling and improve glucose homeostasis.

Afadin depletion under conditions of obesity led to increased circulating insulin levels during a glucose challenge indicating increased insulin secretion from the beta-cells. It was recently shown that β 3-mediated stimulation of WAT lipolysis triggered insulin secretion from the beta-cells [37]. Since Afadin regulates the uptake of fatty acids in adipocytes, the increased insulin secretion observed in FAKO mice could be due to altered lipid metabolism in the adipose tissue consequently regulating beta-cell function. Future studies warrant the involvement of Afadin in lipid utilization.

Insulin-induced phosphorylation of Afadin at S1795 (human S1718) is reduced by insulin resistance and/or obesity in both rodents and human subjects. This indicates that Afadin and its phosphorylation may be directly involved in insulin resistance. However, this occurs despite residual or intact, insulin-induced Akt phosphorylation. Since our data show that Afadin is a negative regulator of insulin action via its phosphorylation on S1795, this implies that reduced Afadin phosphorylation promotes Akt phosphorylation, thereby sustaining functional insulin signaling. Thus, it is tempting to speculate that the phosphorylation of Afadin S1795 acts as an intracellular brake on the insulin pathway which is released during states of accelerated anabolic metabolism such as obesity and insulin resistance. Hence, manipulating Afadin abundance, or its phosphorylation, in adipocytes as a mechanism to enhance insulin action without affecting adiposity could offer a novel therapeutic avenue to treat the alarming increase in insulin resistance and insulin resistance-associated disorders such as T2DM and cardiovascular diseases worldwide.

In conclusion, our findings support a novel role for Afadin, which is not linked to adherens junctions or migration, but to the regulation of signaling cascades and metabolic homeostasis. Our data reveal a novel intracellular negative feedback mechanism regulating insulin action in adipocytes *via* the phosphorylation of Afadin and its interaction with HDAC6, with potential consequences in the pathogenesis of insulin resistance-related disorders.

Materials and Methods

Reagents

Antibodies: Phospho-Afadin (#5485), Total β -actin (#8457), Total β -tubulin (#2128), Acetyl α -tubulin (#5335), Total α -tubulin (#2125), Phospho-Akt (#9271), Total Akt (#9272), Phospho-IGF-1 Receptor β /Insulin Receptor β (#3024), HDAC6 (#7612), acetylated-Lysine (#9441), and Phospho-Erk1/2 (#9102) were from Cell Signaling.

Total I/S-Afadin (A0224), FLAG antibody (F2555), and M2-FLAG magnetic beads (M8823) were from Sigma. Total Insulin Receptor β (sc-57342) was from Santa Cruz. Phospho-TBC1D4 (3028 P1) was from Symansis. Total TBC1D4 (Ab24469) was from Abcam. Macrophage antibody (RM0029-11H3) was from Novus Biologicals.

Chemicals and peptides: Insulin (I9278), T3 (T2877), IBMX (I5879), Dexamethasone (4902), Indomethacin (I7378), FLAG peptide (F3290), *Clostridium Histolyticum* collagenase (C6885), Blastidin (I5205), 2,2,2-Tribromoethanol (T48402), and oil red O solution (O1391) were from Sigma. MK-2206 (A-1206) was from Active Biochem. Tubastatin A (S8049) was from Selleck Chemicals. D-[¹⁴C(U)]-glucose (NEC04B005MC) was from Perkin Elmer. Brilliant III Ultra-fast SYBR Green QPCR Master Mix (600883) was from AH Diagnostics. Lipofectamine[®] RNAiMAX (13778-150), BCA Protein Assay (23223 and 23224), and CHAPS (28300) were from Fisher Scientific.

Oligonucleotides: Mouse primers (TAG Copenhagen) and sgRNA sequences (TAG Copenhagen) are listed in below. MISSION[®] siRNA Universal Negative Control #1 (SIC001), MISSION[®] siRNA, HDAC6 siRNA #1 (SASI_Mm02_00311178), and MISSION[®] siRNA and HDAC6 siRNA #2 (SASI_Mm02_00311179) were from Sigma.

Animal models

All mice were on a C57BL/6J background. Adiponectin-Cre mice were obtained from the Jackson Laboratory (The Jackson Laboratory, Bar Harbor, ME; USA), and *Mllt4^{flox/flox}* mice were provided by Pr. Müller [38]. Mice were housed in the Department of Experimental Medicine, Faculty of Health Sciences, University of Copenhagen at 22°C under daily 12 h light/dark cycles in ventilated racks with cages changed every 2 weeks. For the diet study, mice were given either a 60% fat diet (D12492i, Research Diets) or a sucrose-matched 10% fat diet (D12450Ji, Research Diets) for 16 weeks. All animal experiments were carried out using male mice. See figure legends for age of the mice. For animal experiments involving *Mllt4^{flox/flox}* mice, age-matched littermates were randomly assigned to the experimental groups. *Mllt4^{flox/flox}* female mice were bred with *Mllt4^{flox/flox}* Adipoq-Cre⁺ mice to generate the experimental cohorts.

All animal experiments were approved by the Danish authorities (permit number 2015-15-0201-00728) at the University of Copenhagen (permit number P16-010). For fasting/re-feeding studies, 9-week-old wild-type male mice were fasted overnight. Two groups were allowed access to food *ad libitum* for either 2 or 6 h, respectively. Mice were euthanized; tissues were collected immediately and snap frozen in liquid nitrogen. Insulin injection studies were carried out on mice fasted for 2 h prior to anesthesia with Avertin followed by retro-orbital injection of saline or 1 U insulin. Mice were euthanized after 5 min, and tissues were immediately collected and snap frozen. An independent ambulant cohort was given 0.75 U insulin/kg intraperitoneally (IP) and euthanized either at time 0 (no injection), 15, 60, or 120 min after injection. GTTs and ITTs were performed on mice fasted for 4 h (glucose tolerance test) or 2 h (insulin tolerance test) and injected IP with 1 g glucose/kg body weight or 0.75 U insulin/kg body weight. Blood glucose was measured from the tail bleeding using the Contour XT glucometer.

Glucose-stimulated insulin secretion was done on a cohort of mice after 18 weeks of HFD diet using 2 g/kg body weight.

Plasma insulin levels were measured by ELISA (Mercodia). Time 0 measurements were used to report fasted blood glucose levels. Food intake was recorded by placing mice in single cages and weighing the food before and after a period of 5 days.

Tissue histology

Pieces of tissue were fixed in 4% paraformaldehyde followed by wash in PBS and storage in 70% ethanol. Embedding, sectioning, Sirius Red staining, Macrophage staining, and adipocyte quantifications were done by the University of Copenhagen Core Facility for Integrated Microscopy.

Body composition analysis

Mouse lean and fat mass was measured using nuclear magnetic resonance technology with an EchoMRI 4 in 1 Body Composition Analyzer.

Primary mouse adipocyte isolation

Mature subcutaneous and epididymal fat pads were isolated from 16-week-old euthanized male mice. Subcutaneous fat was minced with scissors in KRPBA buffer (120 mM NaCl, 2.7 mM KCl, 1.2 mM KH₂PO₄, 0.59 mM MgSO₄·7H₂O, 0.87 mM CaCl₂, 14 mM NaHCO₃, 3.5% BSA [W/V%], 6 mM D-Glucose) with 1.5 mg/ml collagenase. Epididymal fat was minced with scissor in HBS buffer (20 mM HEPES-Na pH 7.4, 140 mM NaCl, 5 mM KCl, 2.5 mM MgSO₄, and 1 mM CaCl₂) with 1.5 mg/ml collagenase. Samples were incubated in a shaking water bath at 37°C for 30–40 min. The cell suspension was filtered and mature adipocytes washed twice in respective buffers. Mature subcutaneous adipocytes were used for lipogenesis assay, whereas mature epididymal adipocytes were used for immunoblotting.

Lipogenesis

Equal amounts of washed mature adipocytes were suspended to 10% suspensions in KRPBA buffer in round plastic tubes (10 × 75 mm) containing insulin or vehicle and incubated in a shaking water bath at 37°C for 20 min. 50 μ l KRPBA buffer containing D-[¹⁴C(U)]-glucose was added, and cell suspensions were incubated for 90 min. The tubes were then placed on ice and 1 ml Dole solution (80% 2-propanol, 20% heptane, 2% 1 N H₂SO₄) added followed by vortexing and incubation for 10 min on ice. One ml heptane was added followed by vortexing and incubation for 10 min on ice. Eight hundred μ l of the organic phase was collected in scintillation tubes and allowed to evaporate overnight. Tubes were weighed to quantify amount of lipids (for normalization), and 4 ml scintillation liquid was added. Tubes were vortexed and radioactivity measured on a Hidex 300 SL.

Triglyceride content

iBAT and iWAT were collected and assessed for triglyceride content using a commercial kit from Abnova (Abnova, Germany) using the manufacturer's protocol.

Cell culture

The brown preadipocyte cell-line WT-1 [39] was a kind gift from Dr. C Ronald Kahn. Cells were maintained in DMEM high glucose with 10% fetal bovine serum, 1% Penicillin and Streptomycin (complete media). WT-1 cells were differentiated using the published protocol [39]; briefly, cells were grown to confluence in 20 nM insulin and 1 nM T3. Two days after confluence, cells were induced by adding 20 nM insulin, 1 nM T3, 0.5 mM IMBX, 0.5 μ M Dexamethasone, and 125 mM Indomethacin for 2 days. Cells were then switched back to 20 nM insulin and 1 nM T3 for 4 days with media change every other day. Cells were considered mature 6 days after induction. 3T3-L1 cells (ATCC® CL-173™) were maintained in complete media. Differentiation was induced by adding 5 μ g/ml insulin, 1 μ M Dexamethasone, 0.5 mM IBMX, and 0.5 μ M Rosiglitazone. Two days after, cells were switched to complete media containing 0.5 μ g/ml insulin and 0.5 μ M Rosiglitazone for 2 days, followed by complete media with 0.5 μ M Rosiglitazone. Cells were considered mature after day 6. C2C12 cells (ATCC® CRL-1772™) were cultured in complete media; Hepa-1c1c7 cells (ATCC® CRL-2026™) were cultured in α -MEM with 10% fetal bovine serum, 1% Penicillin and Streptomycin. For insulin stimulation experiments, cells were starved for 3–4 h in DMEM high glucose with 1% Penicillin and Streptomycin and 0.1% bovine serum albumin (BSA). For studies using Tubastatin A, the compound was solubilized in dimethyl sulfoxide (DMSO) and added both during starvation and stimulation. DMSO was used as vehicle in those experiments.

Human immortalized white and brown preadipocytes described and characterized by Xue *et al* [19] were maintained in complete media. Cells were differentiated according to published protocol [40]. Primary human adipocytes were isolated from three male subjects undergoing gastric bypass (average BMI of 41.9 + 1.9) kindly providing a small (~2 × 2 × 3 cm) periumbilical adipose tissue, which were maintained in PBS with BSA in a heating container. Tissue was washed in PBS/BSA followed by dissection with scissors and then collagenase digestion for 15–20 min. The cell suspension was filtered and mature adipocytes collected in 2 ml Eppendorf tubes supplied with 1 ml DMEM. Insulin or vehicle was added for 5 min while tubes were shaking in a water bath at 37°C followed by one wash in ice-cold HBSS and then lysed for immunoblotting.

All subjects approved the procedure and donation of adipose tissue and the Ethics Committee from the Capital Region of Denmark as described in Andersen *et al* [21].

Generation of Afadin KO and mutant expressing cells

The CRISPR/Cas9 system was used to generate Afadin-Knock-Out (KO) cell lines. The Cas9 nickase (nCas9) was used and guide RNAs (sgRNAs) designed using the online tool at <https://zlab.bio/guide-design-resources>. Two different pairs of sgRNAs were designed targeting exon 1 eventually leading to the Af-KO cell-line (sgRNA#1 and sgRNA#2). Within each pair, one sgRNA was cloned into the pX461 (addgene#48140) containing the nCas9 and GFP, and the second sgRNA was cloned into a sgRNA expression cassette according to this protocol [41]. WT-1 cells were electroporated with the plasmid and the expression cassette and sorted according to GFP

intensity 2 days later. Single cell colonies were obtained in 96-wells as well as a bulk of GFP-positive cells. Single cells were grown and analyzed for *Mllt4* invalidation using immunoblotting. Selected clones were further sequenced.

To re-express versions of I-Afadin, the N-terminal FLAG-tagged wild-type (NM_010806.1) or an S1795A version was inserted into the pENTR/D-TOPO plasmid by Genscript. The constructs were cloned into the pLENTI/V5 vector (V533-06, Life Technologies) by LR recombination. Lentivirus was created as previously described [42], and Af-KO cells were transduced. Infected cells were selected using Blasticidin (2.5 μ g/ml). Selection pressure was kept while passaging cells, but not during experimental setups.

Immunoblotting

Cells were starved for 3–4 h prior insulin stimulation for the indicated time points. Cells were then washed once in ice-cold PBS and lysed in lysis buffer A (50 mM HEPES, 150 mM NaCl, 10 mM EDTA, 10 mM Na₄P₂O₇, 100 mM NaF, 1% Triton X-100, 2 mM orthovanadate, and 1% protease inhibitor), followed by centrifugation for 5 min at 16,000 rcf. Supernatant was collected and protein concentration calculated and adjusted using the BCA assay. Lysate was denatured by adding 20% sample buffer (0.35 M Tris-HCl, 30% glycerol, 10% SDS, 603 mM DTT, and 150 μ M bromophenol blue) followed by heating to 95°C for 5 min. Equal amounts of protein were resolved by SDS-PAGE and transferred to polyvinylidene difluoride (PVDF) membranes (Millipore, Denmark). Membranes were blocked in 5% BSA for 1 h followed by overnight incubation with primary antibody in a 1% BSA-TBST solution.

Tissue samples were processed using steel bead homogenization (Tissue Lyser II, Qiagen) in ice-cold lysis buffer B (pH 7.4; 10% glycerol; 1% IGEPAL; HEPES, 50 mM; NaCl, 150 mM; NaF, 10 mM; EDTA, 1 mM; EGTA, 1 mM; sodium pyrophosphate, 20 mM; sodium orthovanadate, 2 mM; sodium pyrophosphate and Sigma protease inhibitors), followed by end-over-end rotation at 4°C for 30 min. Samples were spun down at 16,000 rcf for 15 min, and supernatant was recovered. Preparation of lysates, including adjustment of protein concentrations, SDS-PAGE, and immunoblotting were performed as just described.

Mature adipocytes (mouse or human) were lysed in lysis buffer A followed by end-over-end rotation for 20 min at 4°C. Samples were spun down at 16,000 rcf for 15 min, and supernatant was recovered. Preparation of lysates, SDS-PAGE, and immunoblotting were performed as just described.

Quantified phosphorylations/proteins were normalized to total β -actin, total α / β -tubulin, or total Akt to account for variability in protein loading and transfer during the SDS-PAGE procedure.

Immunoprecipitation

Mature adipocytes lacking endogenous Afadin protein, but re-expressing FLAG-tagged wild-type or S1795A mutant, were starved for 4 h followed by insulin/vehicle treatment for 20 min. Cells were then washed twice in ice-cold PBS and then lysed using different lysis buffers for each experimental setup (a total of four independent experiments). Lysis buffers used: lysis buffer B, lysis

buffer C [Buffer A (20 mM Tris–HCl at pH 7.5, 150 mM NaCl, 1 mM CaCl₂, 1 mM MgCl₂, 1% NP-40, 50 mM NaF, 10 mM β-glycerin, 5 mM NaHPO₄), lysis buffer C but with six washing steps, and lysis buffer D (150 mM KCl, 50 mM HEPES, 1% CHAPS, 2 mM orthovanadate, and 1% protease inhibitor). Cell lysis was incubated end-over-end for 20 min at 4°C, followed by centrifugation for 15 min at 4°C. Supernatant was collected and concentrations adjusted (using the BCA assay). A minimum of 5 mg protein was used per reaction in which 40 μl FLAG-coupled magnetic beads were added. A minor fraction was saved for immunoblotting. Immunoprecipitation occurred by end-over-end at 4°C overnight. Beads were washed three times (except with Lysis buffer C) in the respective lysis buffer followed by resuspension in a surplus of FLAG peptides (according to Manufacturer's protocol). In short, 100 μg/ml FLAG solution was added to the beads followed by end-over-end for 1 h at 4°C. A second elution step was performed after collecting primary elute, by adding a second 100 μg/ml FLAG solution followed by gently shaking at 37°C. Eluate was air-dried by speed-vac, and precipitated proteins were in-gel trypsinized, followed by six-plex TMT labeling and analyzed on an Orbitrap Fusion Mass Spectrometer (The Thermo Fisher Center for Multiplexed Proteomics, Harvard Medical School). Proteins pulled-down in Afadin-ablated cells were considered as background. Immunoprecipitation of IR was done using same conditions, with the exception of adding anti-IR antibodies instead of magnetic beads and adding protein G Sepharose beads (Fisher Scientific) after the overnight incubation followed by end-over-end incubation for 3 h. Elution was carried out by adding sample buffer and heating at 95°C for 5 min.

Immunocytochemistry and images analysis

Mature adipocytes were plated on 0.5% gelatin-coated coverslips, allowed to rest in complete media for 24 h at 37°C. Cells were then starved for 4 h and stimulated with 100 nM insulin for 20 min. Subsequently, cells were fixed with 4% paraformaldehyde, permeabilized with 0.1% Triton X-100, and blocked with 2% BSA in PBS for 1 h. Cells were incubated with antibodies against total insulin receptor β (1:100, Santa Cruz sc-57342) and HDAC6 (1:100, Cell signaling #7558) and appropriate secondary antibodies conjugated to Alexa 488 (green) or Alexa 594 (red) were used. DAPI was used as nuclear counterstain. Fluorescence was examined in Zeiss Confocal microscope LSM 780 with 63 × 1.4 NA oil objective. All images were acquired with exact same settings and with sequential scanning mode. Co-localization analysis was performed in ZEN software subtracting the background and setting appropriate thresholds for each channel. ROI encompassing whole cells were finally used for Manders co-localization coefficients determination [43].

RNA extraction and qPCR analysis

RNA from cultured cells was extracted using the RNeasy kit (74106, Qiagen) and cDNA synthesized using the iScript kit (170-8891, BIO-RAD) according to the manufacturer's instructions. RNA from tissue was extracted using steel bead homogenization in Trizol (Invitrogen). Samples were then incubated for 10 min followed by addition of chloroform and shaking. Samples were centrifuged for 15 min at

12,000 rcf at 4°C. The aqueous phase was retrieved and mixed 1:1 with 70% ethanol. From this step, the samples were transferred to RNeasy columns and this protocol was followed—including DNase treatment. Real-time PCR was performed using the CFX384 Real-Time System according to the supplier's manual (BIO-RAD). Each cDNA sample was run in triplicates. Primer sequences, including primers for genotyping, are described below.

Oil red O

Differentiated cells were washed twice in PBS followed by fixation in 3.7% paraformaldehyde for 30 min. Fixed cells were washed in H₂O and then stained for 30 min in filtered oil red O solution. Lastly, cells were washed to remove any surplus stain.

In vitro fatty acid uptake

Cells were differentiated in 96-wells and starved for 3 h prior to insulin stimulation (100 nM) for 1 h. The QBT fatty acid assay (R8132, Molecular Devices) was then run according to manufacturer's instructions on a Flexstation 3 (Molecular Devices) with readings every 30 s for 1 h. Cells were then washed in PBS, lysed and fatty acid uptake normalized to protein content. Protein lysates were subjected to immunoblotting.

RNA interference in mature adipocytes

Immortalized preadipocytes were differentiated to day 6 and reverse transfected as described by Isidor *et al* [44]. Adipocytes were used 4 days after transfection.

sgRNA sequences

| Oligo | Sequence |
|---------|-------------------------|
| sgRNA#1 | CAGCCGGGCCGGAACACCGCAGG |
| sgRNA#2 | GCGGCCCGCATCATGTCGGCGGG |
| sgRNA#3 | GCTTCCGCCGCTCTTCGTCGCGG |
| sgRNA#4 | CCACTGGAACGCCAACCGGCTGG |

Primers

| Primers for RT–qPCR | | |
|---------------------|------------------------|------------------------|
| Gene | Forward primer | Reverse primer |
| Mllt4 | GGCCTTCTCAAGGGGATGAC | AAAGCTGGTCTCAGGCATGT |
| Cre | GATTCGACCAGGTTTCGTTTC | GCTAACACCGTTTTTCGTTTC |
| 18S | AGTCCCTGCCCTTTGTACACA | GATCCGAGGGCCTCACTAAAC |
| Pparγ2 | GCATGGTGCCTTCGCTGA | TGGCATCTCTGTGTCAACCATG |
| Tbp | ACCCTTACCAATGACTCCTATG | TGACTGCAGCAAATCGTTGG |
| Fabp4 | CTGGGCGTGAATTCGAT | GCTCTTACCTTCTCTGCTGCT |
| C/EBPα | CAAGAACAGCAACGAGTACCG | GCTACTGGTCAACTCCAGCAC |
| C/EBPβ | GGGTTTCGGGACTTGATGC | ACATCAACAACCCCGCAGG |
| PGC1α | CCCTGCCATTGTTAAGACC | TGCTGCTGTTCCTGTTTTTC |
| Elovl3 | GGACTTAAGGCCCTTTTTGG | TTCCGGCTTCTCATGTAGGT |
| IR | GGGCAGATGTACAGAATCAA | CCACCAATACGTCATTCAAC |

Primers (continued)

| Primers for RT-qPCR | | |
|-----------------------------|-------------------------|-------------------------|
| Gene | Forward primer | Reverse primer |
| Plin1 | AGATCCCGGCTCTTCAATACC | AGAACCTTGTCCAGAGGTGCTT |
| Plin2 | GACCTTGTCTCCTCCGCTTAT | CAACCGCAATTTGTGGCTC |
| Plin3 | ATGTCTAGCAATGGTACAGATGC | CGTGGAACTGATAAGAGGCAGG |
| Plin4 | GTGTCCACCAACTCACAGATG | GGACCATTCTTTTGCAGCAT |
| Plin5 | TGTCCAGTCTTACAACCTCGG | CAGGGCACAGGTAGTCACAC |
| Leptin | GCCAGGCTGCCAGAATTG | CTGCCCCCAAGTTTGATG |
| Cidea | ATCACAACTGGCCTGGTTACG | TACTACCCGGTGTCCATTCTT |
| Acadm | GAAACCTGCTCCTTCCACCGA | AACTAAACATGGGCCAGCGA |
| Cpt1b | GTGCTGGAGGTGGCTTTG | TTTGCTGGAGATGTGGAAGA |
| Atgl | TCGTGGATGTTGGTGGAGCT | TGTGGCCTCATTCTCTCTAC |
| Hsl | CACCCATAGTCAAGAACCCTTC | TCTACCCTTTCAGCGTCACCG |
| Mgl | CGGACTTCCAAGTTTTGTGAGA | GCAGCCACTAGGATGGAGATG |
| Sdha | GGAACACTCCAAAAACAGACCT | CCACCACTGGGTATTGAGTAGAA |
| CS (citrate synthase) | GGACAATTTTCCAACCAATCTGC | TCGGTTCATTCCCTCTGCATA |
| Ndufs1 | TTGGGAACAACAGGAAGAGG | TTCCCACTGCATCCATTACA |
| Uqcrb | ACTGGGGTTAATGCGAGATGA | CTGATGCCTCATAGTCAGGTCC |
| Ndufb3 | ATCCATGGGCTCGCAATGAG | AGCTACCACAAACGCAGCAA |
| CytCs | GGTGTCTTTGTGGGGGTGAA | CAAAGTGTCTCCTGTGACCT |
| Cox7c | TTCAGTGAAAAACAAGTGGCG | ACTATAAAGAAAGGTGCGGCA |
| Acaca | CACATCCCATCCAAACAGAG | GCGTTGTCCAACAGAACATC |
| Fasn | ATTGGTGGTGTGGACATGGTC | CCCAGCCTTCCATCTCTCG |
| Scd1 | CCTGCGGATCTTCTTATCA | GTCGCGGTGTGTTTCTGAG |
| Srebp1c | GGAGCCATGGATTGCACATT | GGCCCGGAAGTCACTGT |
| Pck1 | TGGATGTCCGAAGAGGACTT | TGCAGGCACTTGATGAACTC |

Statistics

All data are presented as means + SEM. Comparisons between two groups were done with Student's *t*-test; comparisons between three groups or more were carried out by ANOVA followed by *post hoc* multiple correction tests using GraphPad. *P*-values below 0.05 were considered significant. Hierarchical modeling was done in R to calculate differences in slopes for the ITT.

Data availability

The quantitative co-immunoprecipitation data are available as for each individual replicate as Datasets EV1–EV4.

Expanded View for this article is available online.

Acknowledgements

This work was supported by internal funding from the Novo Nordisk Foundation Center for Basic Metabolic Research, an independent research center at the University of Copenhagen partially funded by an unrestricted donation from the Novo Nordisk Foundation (<http://www.cbmr.ku.dk>), an EFSU/

Lilly European Diabetes Research Programme award and by a grant from the Novo Nordisk Foundation—Endocrinology Research (NNF150C0016510). M.L. was a recipient of a research grant from the Danish Council for Independent Research and Sapere Aude Research Talent: DFF 5053-00112. Y.-H.T. was supported by US National Institutes of Health (NIH) grants R01DK077097 and R01DK102898 (to Y.-H.T.), and P30DK036836 (to Joslin Diabetes Center's Diabetes Research Center, DRC) from the National Institute of Diabetes and Digestive and Kidney Diseases. F.S. was by a grant from American Diabetes Association (#1-18-PDF-169). We thank the members of the Emanuelli group for discussions and the Flow Cytometry Core Facility, University of Copenhagen.

Author contributions

ML and BE designed the study, interpreted the data, and wrote the manuscript. ML, PSSP, MSI, DNMK-S, KP, FS, MT, ELB, and TM performed experiments; EA and VBK isolated and analyzed isolated human adipocytes and SVF. FS and Y-HT provided immortalized human adipocytes and assisted with experiments. CØ performed the histology analysis. UM provided the Mlt4^{flx/flx} mice. RB and ZG-H oversaw critical experiments. All authors approved the article.

Conflict of interest

The authors declare that they have no conflict of interest.

References

- Rosen ED, Spiegelman BM (2014) What we talk about when we talk about fat. *Cell* 156: 20–44
- Gabriely I, Ma XH, Yang XM, Atzmon G, Rajala MW, Berg AH, Scherer P, Rossetti L, Barzilai N (2002) Removal of visceral fat prevents insulin resistance and glucose intolerance of aging: an adipokine-mediated process? *Diabetes* 51: 2951–2958
- Emanuelli B, Vienberg SG, Smyth G, Cheng C, Stanford KI, Arumugam M, Michael MD, Adams AC, Kharitonov A, Kahn CR (2014) Interplay between FGF21 and insulin action in the liver regulates metabolism. *J Clin Invest* 124: 515–527
- Kusminski CM, Holland WL, Sun K, Park J, Spurgin SB, Lin Y, Askew GR, Simcox JA, McClain DA, Li C *et al* (2012) MitoNEET-driven alterations in adipocyte mitochondrial activity reveal a crucial adaptive process that preserves insulin sensitivity in obesity. *Nat Med* 18: 1539–1549
- Wang J, Liu R, Wang F, Hong J, Li X, Chen M, Ke Y, Zhang X, Ma Q, Wang R *et al* (2013b) Ablation of LGR4 promotes energy expenditure by driving white-to-brown fat switch. *Nat Cell Biol* 15: 1455–1463
- Pellegrinelli V, Carobbio S, Vidal-Puig A (2016) Adipose tissue plasticity: how fat depots respond differently to pathophysiological cues. *Diabetologia* 59: 1075–1088
- Hotamisligil GS, Shargill NS, Spiegelman BM (1993) Adipose expression of tumor necrosis factor- α : direct role in obesity-linked insulin resistance. *Science* 259: 87–91
- Hotamisligil GS, Peraldi P, Budavari A, Ellis R, White MF, Spiegelman BM (1996) IRS-1-mediated inhibition of insulin receptor tyrosine kinase activity in TNF- α - and obesity-induced insulin resistance. *Science* 271: 665–668
- Hotamisligil GS (2017) Inflammation, metaflammation and immunometabolic disorders. *Nature* 542: 177–185
- Guilherme A, Virbasius JV, Puri V, Czech MP (2008) Adipocyte dysfunction linking obesity to insulin resistance and type 2 diabetes. *Nat Rev Mol Cell Biol* 9: 367–377

11. Samuel VT, Shulman GI (2012) Mechanisms for insulin resistance: common threads and missing links. *Cell* 148: 852–871
12. Taniguchi CM, Emanuelli B, Kahn CR (2006) Critical nodes in signalling pathways: insights into insulin action. *Nat Rev Mol Cell Biol* 7: 85–96
13. Haeusler RA, McGraw TE, Accili D (2018) Biochemical and cellular properties of insulin receptor signalling. *Nat Rev Mol Cell Biol* 19: 31–44
14. Rabiee A, Kruger M, Ardenkjaer-Larsen J, Kahn CR, Emanuelli B (2018) Distinct signalling properties of insulin receptor substrate (IRS)-1 and IRS-2 in mediating insulin/IGF-1 action. *Cell Signal* 47: 1–15
15. Mandai K, Rikitake Y, Shimono Y, Takai Y (2013) Afadin/AF-6 and canoe: roles in cell adhesion and beyond. *Prog Mol Biol Transl Sci* 116: 433–454
16. Takai Y, Ikeda W, Ogita H, Rikitake Y (2008) The immunoglobulin-like cell adhesion molecule nectin and its associated protein afadin. *Annu Rev Cell Dev Biol* 24: 309–342
17. Xu Y, Chang R, Peng Z, Wang Y, Ji W, Guo J, Song L, Dai C, Wei W, Wu Y et al (2015) Loss of polarity protein AF6 promotes pancreatic cancer metastasis by inducing Snail expression. *Nat Commun* 6: 7184
18. Elloul S, Kedrin D, Knoblauch NW, Beck AH, Toker A (2014) The adherens junction protein afadin is an AKT substrate that regulates breast cancer cell migration. *Mol Cancer Res* 12: 464–476
19. Xue R, Lynes MD, Dreyfuss JM, Shamsi F, Schulz TJ, Zhang H, Huang TL, Townsend KL, Li Y, Takahashi H et al (2015) Clonal analyses and gene profiling identify genetic biomarkers of the thermogenic potential of human brown and white preadipocytes. *Nat Med* 21: 760–768
20. Humphrey SJ, Azimifar SB, Mann M (2015) High-throughput phosphoproteomics reveals *in vivo* insulin signaling dynamics. *Nat Biotechnol* 33: 990–995
21. Andersen E, Ingerslev LR, Fabre O, Donkin I, Altintas A, Verstehey S, Bisgaard T, Kristiansen VB, Simar D, Barres R (2018) Preadipocytes from obese humans with type 2 diabetes are epigenetically reprogrammed at genes controlling adipose tissue function. *Int J Obes* 43: 306–318
22. Ran FA, Hsu PD, Lin CY, Gootenberg JS, Konermann S, Trevino AE, Scott DA, Inoue A, Matoba S, Zhang Y et al (2013a) Double nicking by RNA-guided CRISPR Cas9 for enhanced genome editing specificity. *Cell* 154: 1380–1389
23. Mandai K, Nakanishi H, Satoh A, Obaishi H, Wada M, Nishioka H, Itoh M, Mizoguchi A, Aoki T, Fujimoto T et al (1997) Afadin: a novel actin filament-binding protein with one PDZ domain localized at cadherin-based cell-to-cell adherens junction. *J Cell Biol* 139: 517–528
24. Mandai K, Nakanishi H, Satoh A, Takahashi K, Satoh K, Nishioka H, Mizoguchi A, Takai Y (1999) Ponsin/SH3P12: an I-afadin- and vinculin-binding protein localized at cell-cell and cell-matrix adherens junctions. *J Cell Biol* 144: 1001–1017
25. Qian H, Chen Y, Nian Z, Su L, Yu H, Chen FJ, Zhang X, Xu W, Zhou L, Liu J et al (2017) HDAC6-mediated acetylation of lipid droplet-binding protein CIDEC regulates fat-induced lipid storage. *J Clin Invest* 127: 1353–1369
26. Valenzuela-Fernandez A, Cabrero JR, Serrador JM, Sanchez-Madrid F (2008) HDAC6: a key regulator of cytoskeleton, cell migration and cell-cell interactions. *Trends Cell Biol* 18: 291–297
27. Zhang Y, Kwon S, Yamaguchi T, Cubizolles F, Rousseaux S, Kneissel M, Cao C, Li N, Cheng HL, Chua K et al (2008) Mice lacking histone deacetylase 6 have hyperacetylated tubulin but are viable and develop normally. *Mol Cell Biol* 28: 1688–1701
28. Butler KV, Kalin J, Brochier C, Vistoli G, Langley B, Kozikowski AP (2010) Rational design and simple chemistry yield a superior, neuroprotective HDAC6 inhibitor, tubastatin A. *J Am Chem Soc* 132: 10842–10846
29. Murakami K, Eguchi J, Hida K, Nakatsuka A, Katayama A, Sakurai M, Choshi H, Furutani M, Ogawa D, Takei K et al (2016) Antiobesity action of ACAM by modulating the dynamics of cell adhesion and actin polymerization in adipocytes. *Diabetes* 65: 1255–1267
30. Shin CS, Lecanda F, Sheikh S, Weitzmann L, Cheng SL, Civitelli R (2000) Relative abundance of different cadherins defines differentiation of mesenchymal precursors into osteogenic, myogenic, or adipogenic pathways. *J Cell Biochem* 78: 566–577
31. Tran KV, Gealekman O, Frontini A, Zingaretti MC, Morroni M, Giordano A, Smorlesi A, Perugini J, De MR, Sbarbati A et al (2012) The vascular endothelium of the adipose tissue gives rise to both white and brown fat cells. *Cell Metab* 15: 222–229
32. Lin WH, Huang CJ, Liu MW, Chang HM, Chen YJ, Tai TY, Chuang LM (2001) Cloning, mapping, and characterization of the human sorbin and SH3 domain containing 1 (SORBS1) gene: a protein associated with c-Abl during insulin signaling in the hepatoma cell line Hep3B. *Genomics* 74: 12–20
33. Choudhary C, Kumar C, Gnad F, Nielsen ML, Rehman M, Walther TC, Olsen JV, Mann M (2009) Lysine acetylation targets protein complexes and co-regulates major cellular functions. *Science* 325: 834–840
34. Pirola L, Zerzaihi O, Vidal H, Solari F (2012) Protein acetylation mechanisms in the regulation of insulin and insulin-like growth factor 1 signalling. *Mol Cell Endocrinol* 362: 1–10
35. Wang CF, Zhang G, Zhao LJ, Qi WJ, Li XP, Wang JL, Wei LH (2013a) Overexpression of the insulin receptor isoform A promotes endometrial carcinoma cell growth. *PLoS One* 8: e69001
36. Nagarajan A, Petersen MC, Nasiri AR, Butrico G, Fung A, Ruan HB, Kursawe R, Caprio S, Thibodeau J, Bourgeois-Daigneault MC et al (2016) MARCH1 regulates insulin sensitivity by controlling cell surface insulin receptor levels. *Nat Commun* 7: 12639
37. Heine M, Fischer AW, Schlein C, Jung C, Straub LG, Gottschling K, Mangels N, Yuan Y, Nilsson SK, Liebscher G et al (2018) Lipolysis triggers a systemic insulin response essential for efficient energy replenishment of activated brown adipose tissue in mice. *Cell Metab* 28: 644–655
38. Gil-Sanz C, Landeira B, Ramos C, Costa MR, Muller U (2014) Proliferative defects and formation of a double cortex in mice lacking Mlth4 and Cdh2 in the dorsal telencephalon. *J Neurosci* 34: 10475–10487
39. Fasshauer M, Klein J, Kriaciunas KM, Ueki K, Benito M, Kahn CR (2001) Essential role of insulin receptor substrate 1 in differentiation of brown adipocytes. *Mol Cell Biol* 21: 319–329
40. Shamsi F, Tseng YH (2017) Protocols for generation of immortalized human brown and white preadipocyte cell lines. *Methods Mol Biol* 1566: 77–85
41. Ran FA, Hsu PD, Wright J, Agarwala V, Scott DA, Zhang F (2013b) Genome engineering using the CRISPR-Cas9 system. *Nat Protoc* 8: 2281–2308
42. Lundh M, Plucinska K, Isidor MS, Petersen PSS, Emanuelli B (2017) Bidirectional manipulation of gene expression in adipocytes using CRISPRa and siRNA. *Mol Metab* 6: 1313–1320
43. Manders E, Verbeek F, Aten J (1993) Measurement of co-localization of objects in dual-colour confocal images. *J Microsc* 169: 375–382
44. Isidor MS, Winther S, Basse AL, Petersen MC, Cannon B, Nedergaard J, Hansen JB (2016) An siRNA-based method for efficient silencing of gene expression in mature brown adipocytes. *Adipocyte* 5: 175–185